Available online at www.sciencedirect.com

ScienceDirect

Ceramics International 40 (2014) 3277–3285

CERAMICS INTERNATIONAL

www.elsevier.com/locate/ceramint

Deposition of thin ultrafiltration membranes on commercial SiC microfiltration tubes

Marco Facciotti[a], Vittorio Boffa[a,*], Giuliana Magnacca[b], Lars Bjerg Jørgensen[a], Peter Kjær Kristensen[c], Ali Farsi[a], Katja König[a], Morten Lykkegaard Christensen[a], Yuanzheng Yue[a]

[a] *Section of Chemistry, Aalborg University, DK-9000 Aalborg, Denmark*
[b] *Dipartimento di Chimica, Universitá di Torino, 10125 Torino, Italy*
[c] *Department of Physics and Nanotechnology, Aalborg University, DK-9220 Aalborg, Denmark*

Received 23 September 2013; accepted 24 September 2013
Available online 1 October 2013

Abstract

Porous SiC based materials present high mechanical, chemical and thermal robustness, and thus have been largely applied to water-filtration technologies. In this study, commercial SiC microfiltration tubes with nominal pore size of 0.04 μm were used as carrier for depositing thin aluminum oxide (Al_2O_3) ultrafiltration membranes. These ultrafiltration membranes were obtained by coating, drying and calcination of a colloidal suspension of boehmite particles. After calcination, the membrane material consisted of nanosized γ-Al_2O_3 crystallites and had a narrow pore size distribution with average pore size of 5.5 nm. Membrane thickness was tuned by repeating the coating of boehmite sol. By doing so, we were able to reduce the defect density on the membrane surface, as evidenced by SEM analysis and by the significant reduction of water permeance after depositing the second γ-Al_2O_3 layer. After five times coating, a 5.6 μm thick γ-Al_2O_3 layer was obtained. This membrane shows retention of ~75% for polyethylene glycol molecules with M_n of 8 and 35 kDa, indicating that, despite their intrinsic surface roughness, commercial SiC microfiltration tubes can be applied as carrier for thin ultrafiltration membranes. This work also indicates that an improvement of the commercial SiC support surface smoothness may greatly enhance permeance and selectivity of γ-Al_2O_3 ultrafiltration membranes by allowing the deposition of thinner defect-free layers.

Keywords: Silicon carbide; Aluminum oxide; Ultrafiltration; Sol–gel

1. Introduction

Membrane processes are known to have high energy-efficiency and the substitution of the traditional separation systems, as crystallization, distillation, and adsorption, with membrane units is expected leading to vast energy savings [1–3]. In this context, porous ceramic membranes have attracted considerable attention, since they present higher mechanical, chemical, and thermal robustness than their polymeric counterparts [4]. In past years ceramic membranes have been proposed for a broad application spectrum, encompassing water cleaning [5,6] membrane reactors [7,8], and gas purification technologies [9–11]. Among them, ultrafiltration is at present the most interesting application from an industrial prospective, because ultrafiltration membranes can be used for water remediation [12], the recovery of surfactants in industrial cleaning [13], and the concentration and purification of drugs, fruit juices, and natural products [14–17].

Mesoporous γ-alumina (γ-Al_2O_3) was one of the first ceramic materials being selected for the fabrication of ceramic ultrafiltration membranes [18,19]. γ-Al_2O_3 films with large surface area, large pore volume, and narrow pore size distribution in the mesopore range can be prepared by coating, drying and calcination of boehmite (AlOOH) colloidal suspensions [20]. Because of these features, γ-Al_2O_3 membranes are broadly used in liquid filtration or as support for microporous (pore $\varnothing < 2$ nm [21]) gas-selective layers [1]. However, the optimization of these membranes is still under investigation [3,22]. These membranes are usually coated on the α-alumina macroporous (pore $\varnothing > 50$ nm [21]) supports, which are chemically stable, but rather brittle. Moreover, they have a

---

[*] Corresponding author. Tel.: +45 99403579; fax: +45 96350558.
E-mail address: vb@bio.aau.dk (V. Boffa).

0272-8842/$ - see front matter © 2013 Elsevier Ltd and Techna Group S.r.l. All rights reserved.
http://dx.doi.org/10.1016/j.ceramint.2013.09.107

small specific pore volume, and therefore oppose high resistance to the permeate flow. In many cases, the resistance of the α-Al_2O_3 support has been reported to be comparable to [23] or higher than the coated γ-Al_2O_3 active layer [24,25]. The use of more robust and porous supports is expected to enhance the overall performances of composite γ-Al_2O_3 membranes [2,26]. Thus, alternative supports with higher mechanical resistance and porosity are still being developed, e.g. porous stainless steel substrates [3].

In this study, commercial silicon carbide (SiC) microfiltration tubes are tested as carrier for ultrafiltration γ-Al_2O_3 membranes. SiC is a highly covalent material with high hardness and chemical stability [27,28]. SiC microfiltration membranes have been reported to have exceptionally high water-permeability [29] and to be stable in a broad pH and temperature range [30]. Moreover, SiC membranes are exceptionally hydrophilic and exhibit low reversible and irreversible fouling when compared to the other ceramic and polymeric membranes [31]. Fig. 1a shows the picture of a commercial SiC membrane tube. This type of membranes is normally prepared from preformed particles by liquid or vapor phase sintering [32]. The membrane depicted in Fig. 1 consists of several porous SiC layers with progressively smaller pore size (Fig. 1b) down to 40 nm, i.e., the nominal pore size of the inner membrane layer.

These membranes have already been applied to the concentration of sludge, to water sterilization and to treat Produced water. In this work we explore whether these commercial SiC microfiltration membranes can be used as carrier for the deposition of a thin γ-Al_2O_3 ultrafiltration membrane with pore size < 10 nm. Despite their high chemical stability and water permeability, SiC microfiltration membranes have been considered as membrane supports only in a few cases, which mostly concern the fabrication of amorphous SiC membranes [33,34]. Due to their dense structure, such membranes are permeable to small gas molecules such as helium and hydrogen, but not to liquid substances, and therefore they are not suitable for application in the ultra- or nanofiltration range.

So far, SiC microfiltration tubes have not been really considered as supports for ultrafiltration membranes, probably due to their high surface roughness that makes difficult to coat thin defect-free ceramic layers on them. Fig. 1c shows a SEM image of the internal surface of the commercial membrane depicted in Fig. 1a and b. SiC grains emerge from the membrane surface forming sharp mountains and valleys with a modulation of 0.2–1 μm. This type of surface roughness depends on the size of the SiC grains used for the fabrication of this material and on the crystal growth occurring during high temperature fabrication. The deposition of a thin layer on the surface of such support is expected to be a great challenge. Despite that, these supports are here considered as carriers for the deposition of ultrafiltration membranes, since, to the best of our knowledge, SiC microfiltration membranes with a smoother surface are not commercially available.

In this work, the γ-Al_2O_3 layers with different thicknesses will be fabricated by multiple coating and characterized by measuring their retention of a series of poly(ethylene glycol) molecules with different molecular masses. This technique has been applied, because the rejection curves of the support and of the membranes can easily be determined and compared with this method [35–37], and because it allows forecasting to a certain extent the separation performances of the membrane.

2. Materials and methods

2.1. Materials

Aluminum-tri-sec-butoxide (97% purity) and concentrated nitric acid (70%) used for the boehmite sol synthesis were purchased from Sigma-Aldrich. Polyvinyl alcohol ($M_W = 72000$ g/mol) used as a binder in the boehmite coating was obtained from Merck (Darmstadt, Germany). SiC microfiltration tubes with internal diameter of 19 ± 1 mm, length of 305 ± 1 mm and nominal pore size of ~ 0.04 μm, were kindly provided by LiqTech International A/S (Ballerup, Denmark). These SiC tubes were used as supports for membrane deposition. Poly(ethylene glycol) (PEG) with average molecular weight (number average, M_n) of 1, 8, and 35 kD was purchased from Sigma-Aldrich. Deionized water (conductivity < 1.5 μS cm^{-1} at 25 °C) was used for all the preparations and the filtration tests that are described in this work.

2.2. Membrane fabrication

A boehmite sol was synthesized following a known procedure [18]. Aluminum-tri-sec-butoxide was dropped in double-distilled water under vigorous stirring at 96 °C. The molar ratio

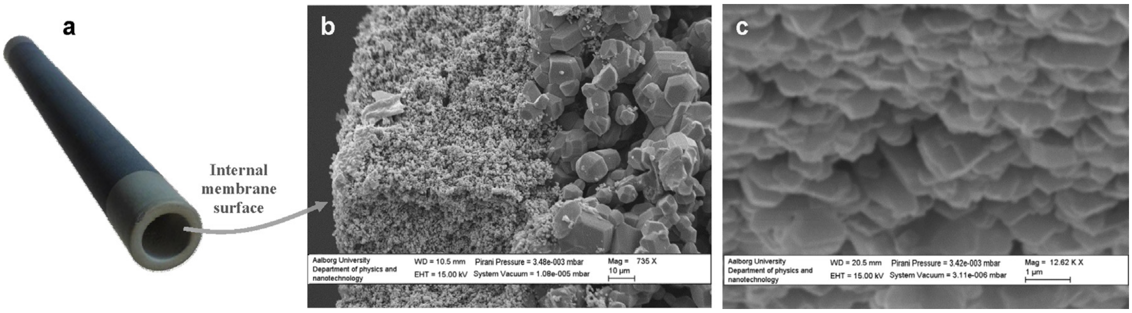

Fig. 1. Photo of a SiC membrane monotube with the nominal pore size of 0.04 μm (Liqtech International A/S, Denmark) (a), and its SEM images: cross-section (b) and SiC grains of the internal membrane surface (c).

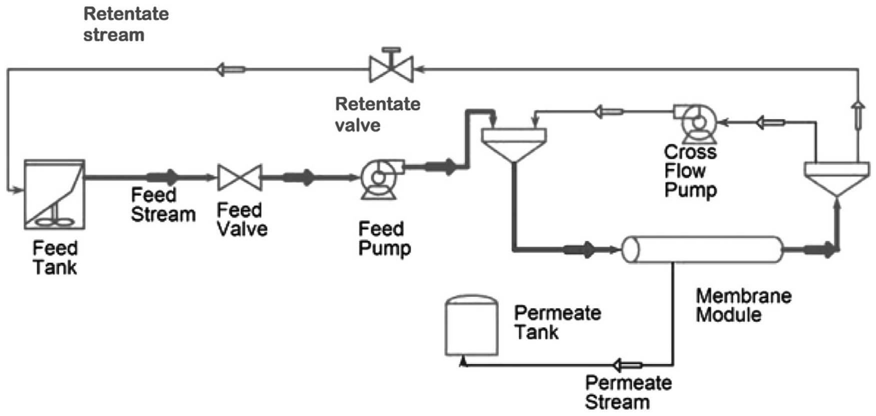

Fig. 2. Schematic diagram of the apparatus used in this study for filtration experiments.

between the aluminum oxide precursor and water was 1:140. The mixture was kept at 96 °C for 4 h to allow alcohol formed by the hydrolysis of metal alkoxide to evaporate, and then the mixture was cooled down to 60 °C. The volume of the evaporated solvent was partially compensated by adding water to obtain a 0.5 M boehmite suspension. The sol was stabilized by adding concentrated nitric acid till a pH equal to 2.8 was reached, followed by refluxing for 20 h. The final product was a bluish transparent boehmite sol. A 30 g L^{-1} solution of PVA in 0.05 M nitric acid was added to the sol in a 2:3 volume ratio. Membranes were coated vertically on a lab-made machine at a dipping/withdrawing rate of 1.5 cm min^{-1}. After coating, membranes were dried at 25 °C in a close box (volume ~ 2 L) at room temperature for 3 h, and then calcined in air at 600 °C for 3 h (at a heating/cooling rate of 2 °C min^{-1}). This coating procedure was repeated zero, one and four times on different supports to obtain γ-Al_2O_3 membranes of different thicknesses.

2.3. Membrane characterization

The particle size distribution of the boehmite sol was determined by dynamic light scattering (DLS) analysis on a Zetasizer Nano NS (Malvern, UK). Unsupported membranes were prepared by drying the boehmite sols in the air, and calcining the deriving powder under the same condition used for the supported samples. The crystal structure of the synthesized material was determined by X-ray diffraction (XRD) on a PANalytical Empyrean diffractometer (Almelo, The Netherlands) operating at 45 kV and 40 mA, with Ni-filtered Cu Kα radiation ($\lambda = 1.5418$ Å). HighScore software by PANalytical was used to analyze the XRD data and to determine the crystal structure of the sample. Porosity and specific surface area were measured on about 0.2 g of unsupported sample by means of N_2 adsorption at liquid-nitrogen boiling point in a gas-volumetric apparatus (ASAP2020 model by Micromeritics). Prior to analysis, samples were outgassed in vacuum (residual pressure $\sim 10^{-5}$ bar) at 373 K for 8 h, in order to avoid undesired interferences of gaseous products from materials during the gas-volumetric determinations. Surface areas were calculated by means of the BET model. Pore volumes and pore size distributions were calculated by using the Barret–Joyner–Halenda (BJH) method applied to the entire adsorption branch of the isotherm.

2.4. Filtration tests

Water and PEG permeation measurements were carried on a stainless steel filtration apparatus, the scheme of which is depicted in Fig. 2. In all the experiments, the pressure was controlled by manually adjusting the retentate valve. Water permeation experiments were performed with deionized water, at a cross-flow velocity of 1.1 m s^{-1} and at a trans-membrane pressure ≤ 10 bar. Permeate mass was recorded during filtration over a balance connected to a PC, while retentate was recycled in the feed tank. The same operational conditions were used for the PEG retention measurements. In this case, a feed solution was prepare by dissolving 10 g of PEG powder with average mass (M_n) equal to 1 kDa, 10 g of PEG with $M_n = 8$ kDa, and 10 g of PEG with $M_n = 35$ kDa in 10 L of deionized water. Permeate, feed, and retentate samples were collected simultaneously after fixed periods of time. The filtration setup was flushed with 15 L of deionized water before and after each PEG filtration experiment.

2.5. PEG retention analysis

The concentration of the PEG in the feed, permeate and retentate was determined using a size-exclusion chromatographic column (SEC) interfaced to an evaporative light scattering detector (ELSD). Samples were injected by a Dionex ASI-100 Automated Sample Injector in a PolySep GFC-P 4000 column in a Varian 380-LC apparatus. The signal intensity measured by the ELSD detector is known to follow a non-linear trend with the concentration. Therefore before each measurement, a calibration curve was obtained by fitting a fourth-order polynomial equation on the ELSD intensity data concerning 12 solutions obtained by volumetric dilution of the membrane feed solution. Samples collected during the filtration experiments were directly injected in the column, without further filtration. Peak integration was performed by the Newton–Cotes trapezoid rule.

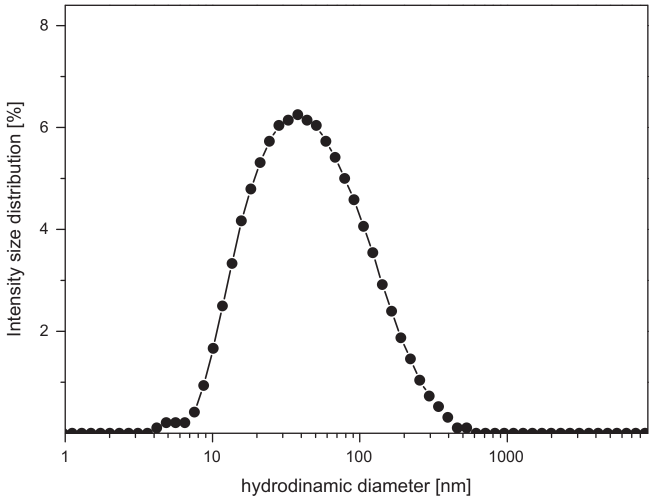

Fig. 3. Particle size distribution of boehmite sol as measured by dynamic light scattering (DLS) analysis.

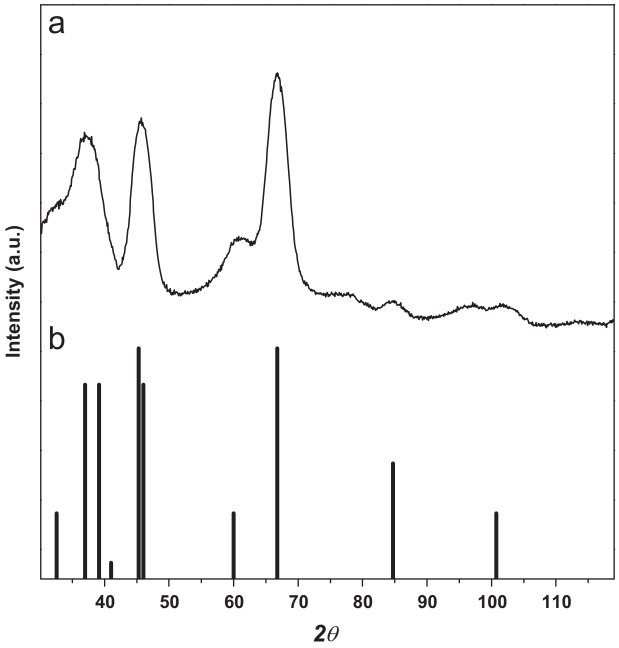

Fig. 4. XRD pattern of the membrane powder after calcination at 600 °C (a) and of a γ-Al_2O_3 reference [39] (b).

3. Results and discussion

3.1. Membrane fabrication

Sol–gel deposition of ceramic thin films on the surface of a macroporous support is not trivial. Indeed, the formation of a defect-free layer with defined pore structure depends on particles morphology, sol rheology, and coating procedure. A boehmite sol was synthesized following the procedure reported in Section 2. Fig. 3 shows the hydrodynamic diameter distribution of the particle of this sol, as measured by DLS analysis after filtration on a 0.8 μm filter. The boehmite sol shows a narrow particle size distribution with mean of about 35 nm. Particles with such a distribution appear to be suitable for coating on the commercial SiC tube in Fig. 1, since they can form a layer without being drained into its pores. Furthermore, this particle size distribution is expected to yield a consolidated membrane with porosity suitable for ultrafiltration applications [20]. Substrate roughness and capillary forces exerted by the substrate pores during drying can easily result in film cracking [38]. Therefore, polyvinyl alcohol (PVA) was used to change the sol rheology and the viscoelastic properties of the dried film.

3.2. Membrane morphology

A sample of the PVA–boehmite sol was dried in air and calcined for 3 h at 600 °C to form an unsupported membrane, which was used for material characterization. Crystallographic phase identification was attained by XRD analysis. The diffractogram of the membrane powder after calcination is depicted in Fig. 4a. The broad peaks indicate a poorly crystalized structure and small crystallite size, which is common for sol–gel derived material calcined at this temperature and is consistent with the small size of the initial sol particles. The crystalline phase of the synthesized membrane is identified to be γ-Al_2O_3, since a good correspondence was found between the position of the peak maxima in Fig. 4a and the XRD pattern of a reference γ-Al_2O_3 sample [39] in Fig. 4b.

The nitrogen sorption data of the unsupported γ-Al_2O_3 membrane after calcination at 600 °C are depicted in Fig. 5. The shape of the sorption curve and the presence of a large hysteresis loop (Fig. 5a) allow to classify the isotherm as a type IV of IUPAC definition [40], which corresponds to a truly mesoporous material. From the analysis of this sorption isotherm, the specific surface area has been calculated to be 205 $m^2\ g^{-1}$, which is consistent with the values reported in literature for other sol–gel derived γ-Al_2O_3 materials [18–26]. The pore size distribution depicted in Fig. 5b was calculated from the adsorption branch by applying the BJH method. The unsupported γ-Al_2O_3 membrane has a narrow distribution of pore width, with a mean value of 5.5 nm. A material with such pore size distribution is the results of the strictly controlled experimental conditions applied to the synthesis, dispersion, and filtration steps [3], and is suitable for the fabrication of ultrafiltration membranes [24,25].

Fig. 6 shows the SEM image of the bare SiC support and of γ-Al_2O_3 membranes that were obtained by one, two and five times repeated coating with the boehmite sol. Notwithstanding the intrinsic surface roughness of the support material, a continuous γ-Al_2O_3 layer of ~0.3 μm thickness was obtained after the first coating (Fig. 6a). However, this layer has inhomogeneous thickness and its surface presents the modulation of the underneath support grains. Moreover, microdefects are visible on the membrane surface, as the pin-hole indicated by the arrow in the picture. After a second coating, a smooth γ-Al_2O_3 layer with 1.3 ± 0.4 μm thickness was formed (Fig. 6b). Fig. 6c shows the γ-Al_2O_3 formed on a different support after

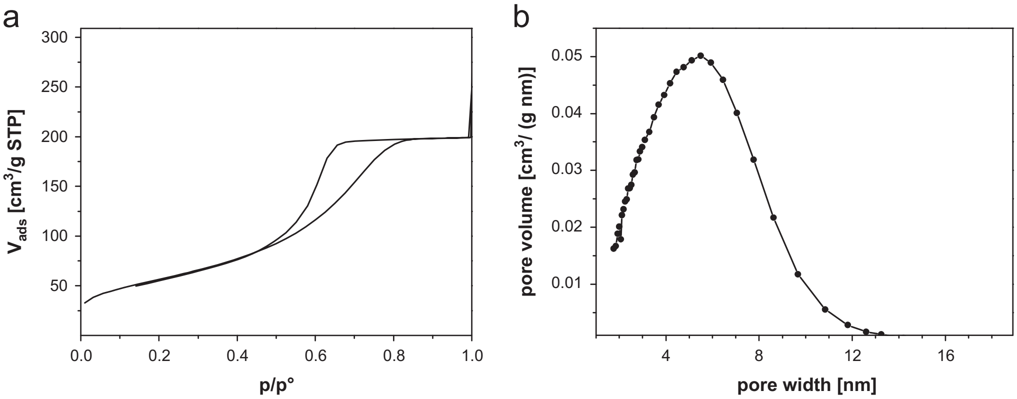

Fig. 5. Nitrogen sorption isotherm (A) of the γ-Al_2O_3 unsupported membrane and the correspondent pore size distribution (B), obtained from the adsorption branch by applying the BHJ method.

five times coating. The membrane has thickness of 5.6 ± 0.4 μm and its surface is smooth and does not show the modulation of the SiC grains of the underneath support. The presence of spin–holes in this layer was not revealed by SEM analysis.

3.3. Water permeability

The permeance of pure water was measured for the bare SiC support and for the coated γ-Al_2O_3 membranes. Permeance values obtained under the steady-state are shown in Fig. 7 as a function of the active layer thickness. The bare SiC microfiltration support presents a water permeance of 8.1×10^3 L $(m^2 \text{ h bar})^{-1}$. This permeance value is remarkably higher than those typically measured for defect-free α-Al_2O_3 support, commonly smaller than 10^2 L $(m^2 \text{ h bar})^{-1}$. This exceptionally high water permeability can be ascribed to the combination of the high pore volume (45%) and the hydrophilicity of the macroporous material forming the support.

γ-Al_2O_3 has lower pore volume, much smaller pore size, and higher pore tortuosity than the support material. Therefore the γ-Al_2O_3 layer can oppose significantly higher resistance to water permeation than the support. In spite of this, the water permeance of the membrane has decreased only three-fold after the first γ-Al_2O_3 coating (thickness = 0.3 μm). This observation is consistent with the large number of defects observed in this membrane layer by SEM analysis. On the contrary, the water permeance of the membrane has further dropped by one order of magnitude after the second γ-Al_2O_3 coating, indicating that many defects in the filtering top-layer were cured by repeating the coating procedure.

A water permeance of 9 L $(m^2 \text{ h bar})^{-1}$ was measured for the 5.6 μm thick membranes, for which the coating procedure was repeated five times. This value is about 900 times lower than the permeance measured for the bare support. Nevertheless, the water permeance measured for this membrane is still higher than that reported in literature for γ-Al_2O_3 membranes on porous α-Al_2O_3 supports, commonly <5 L $(m^2 \text{ h bar})^{-1}$ [2] also for membranes with a thinner active layer.

3.4. PEG retention

A single-step filtration method of polyethylene glycols (PEG) was developed and used to characterize the membranes fabricated in this study. A solution containing three PEG with different molecular weights was prepared in deionized water. The molecular weight of the starting PEG powders was selected in order to allow a good peak resolution during analysis by size-exclusion chromatography. Fig. 8 shows the chromatograms of feed, retentate, and permeate corresponding to the filtration of an aqueous solution of the PEG mixture on the 5.6 μm thick γ-Al_2O_3 membrane. All chromatograms show three peaks at a retention time of about 6, 7 and 8 min, which were assigned to the PEG with nominal molecular mass equal to 35, 8 and 1 kDa, respectively. Feed and retentate have similar chromatograms. This can be explained by the fact that, as typical for ultrafiltration experiments, the permeation rate of water through the membrane is rather low compared to the feed cross-flow velocity, and therefore considerably high concentration of the feed can be achieved only for long filtration times. On the contrary, the intensity of the three chromatographic peaks is significantly lower for the permeate sample than for the feed and the retentate samples, indicating that the γ-Al_2O_3 top-layer can actually retain the dissolved PEG molecules. PEG concentration in the filtration streams was determined from the chromatographic peaks as described in Section 2.

PEG filtration was performed over 2 h on the SiC support and for the three γ-Al_2O_3 membranes. In all cases, the steady state was reached after less than 30 min, after which the concentrations of the three PEG in the feed, permeate and retentate streams were constant. Membrane retention under the steady state was determined for each PEG, according to the following equation:

$$R\,(\%) = \left(1 - \frac{C_p}{C_f}\right) \times 100 \qquad (1)$$

where R, C_p, and C_f are the retention, the concentration in the permeate, and the concentration in the feed, respectively, of a PEG with a specific molecular weight.

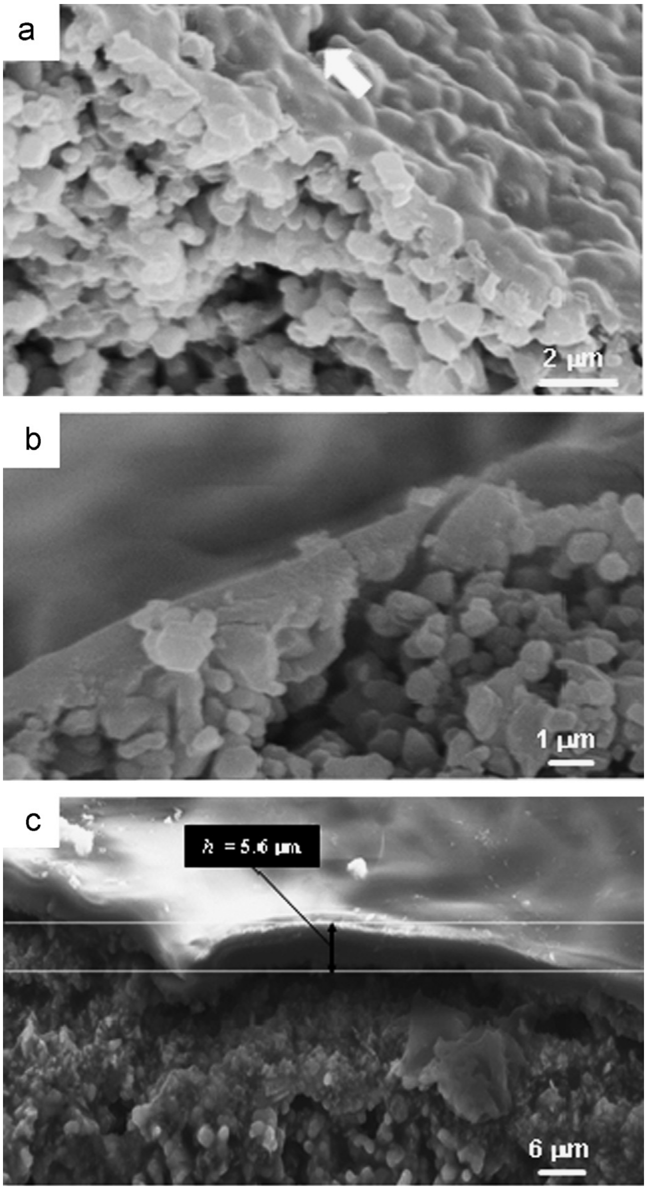

Fig. 6. SEM picture of γ-Al_2O_3 membranes on macroporous SiC tubes. The coating procedure was repeated one (a); two (b) and five times (c), yielding membranes with different thicknesses. The white arrow in the top image indicates a pin-hole in the thin γ-Al_2O_3 layer. The two horizontal lines in the bottom image help the reader to visualize the membrane thickness.

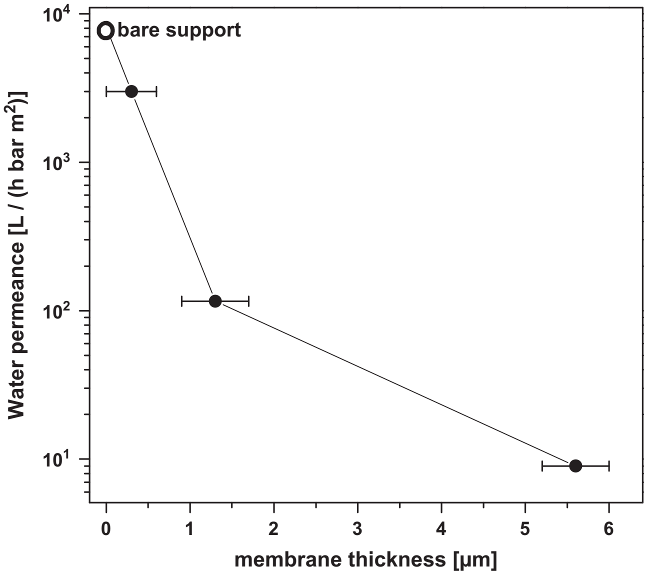

Fig. 7. Water permeance of the bare SiC tube and of the supported ultrafiltration membranes as function of the γ-Al_2O_3 layer thickness. Permeance values, were measured at a trans-membrane pressure of 1 bar for the naked support and the 0.3 μm thick γ-Al_2O_3 layer, and of 10 bar for the other two membranes.

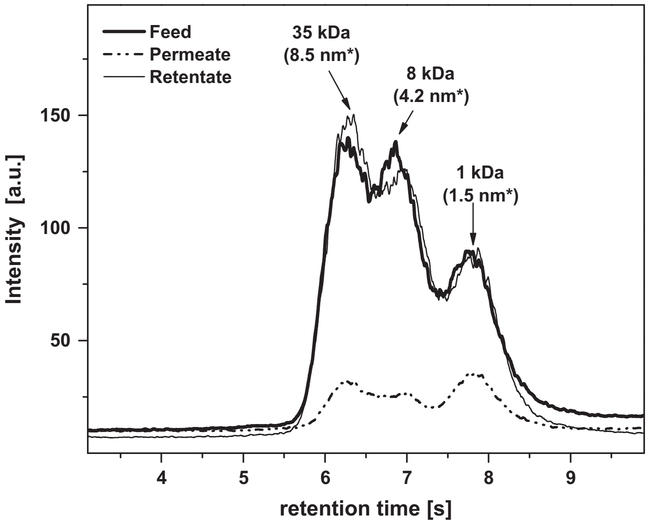

Fig. 8. Chromatograms of the feed, retentate, and permeate samples obtained during the filtration of a PEG solution on the 5.6 μm thick γ-Al_2O membrane. *The diameter of the PEG molecules was estimated from their average molecular mass [42].

Fig. 9 shows the calculated retention, R, as a function of the theoretical hydrodynamic diameter of the PEG probes, estimated from their molecular weight as reported elsewhere [42]. As expected, the commercial SiC macrofiltration membrane has too large pores to retain any of the dissolved PEG polymers. Also the membrane coated once with a γ-Al_2O_3 layer presents negligible PEG retention. This result is consistent with an ultrafiltration layer presenting high defect density, as revealed by SEM analysis and by the high water permeance of this membrane. On the contrary, after the second coating (1.3 μm thick layer) an average retention of 18% was measured for the three PEGs. After repeating the membrane coating five times (5.6 μm thick layer), the PEG retention consistently increased reaching 66% for the PEG with hydrodynamic diameter 1.5 nm ($M_n = 1$ kDa) and ~75% for the PEGs with larger size, namely 4.2 nm ($M_n = 8$ kD) and 8.5 nm ($M_n = 35$ kD). Therefore, the perm-selectivity of the 5.6 μm thick γ-Al_2O_3 membrane is already interesting for practical applications. The difference in retention among the smallest and the two largest PEGs suggests that the membrane has a molecular weight cut-off (MWCO) between 1 and 7 kDa, and a main membrane pore size between 2 and 4 nm. This result is consistent with literature data, showing a MWCO of 2–7 kDa

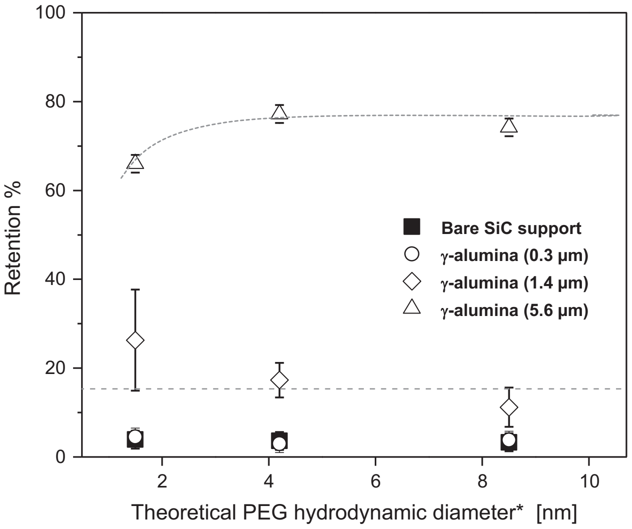

Fig. 9. Retention as function of the PEG hydrodynamic diameter for the bare support and the γ-Al_2O_3 membrane analyzed in this study. *The hydrodynamic diameter of the PEG molecules was estimated from their average molecular mass [42].

for γ-Al_2O_3 membranes [2]. However, this also suggests that the alumina membrane coated on the SiC tube has slightly narrower pores than the unsupported one, for which a mean pore width of 5.5 nm was measured by nitrogen adsorption. On the other hand, it is well known that different characterization techniques can yield slightly different pore size distributions. It is also reasonable that membrane pores should have significantly larger size than the PEG probe to observe an appreciable permeation [43].

The retention of the two largest PEG was ~75%, and not >90% as expected for a defect free γ-Al_2O_3 membrane. A close look at the support (Fig. 10a) reveals the presence of a small number of craters and large SiC grains and aggregates emerging from the support surface. The presence of these defects might not affect the separation performance of the microfiltration SiC support, but introduces cusps and points with high surface curvature, making more challenging the coating. Fig. 10b and c show the presence of microcracks in the γ-Al_2O_3, occurring just in correspondence of these inhomogeneities. These microcracks affect the selectivity of the final membrane and cannot be cured even by coating several γ-Al_2O_3 layers on the internal surface of the membrane tube.

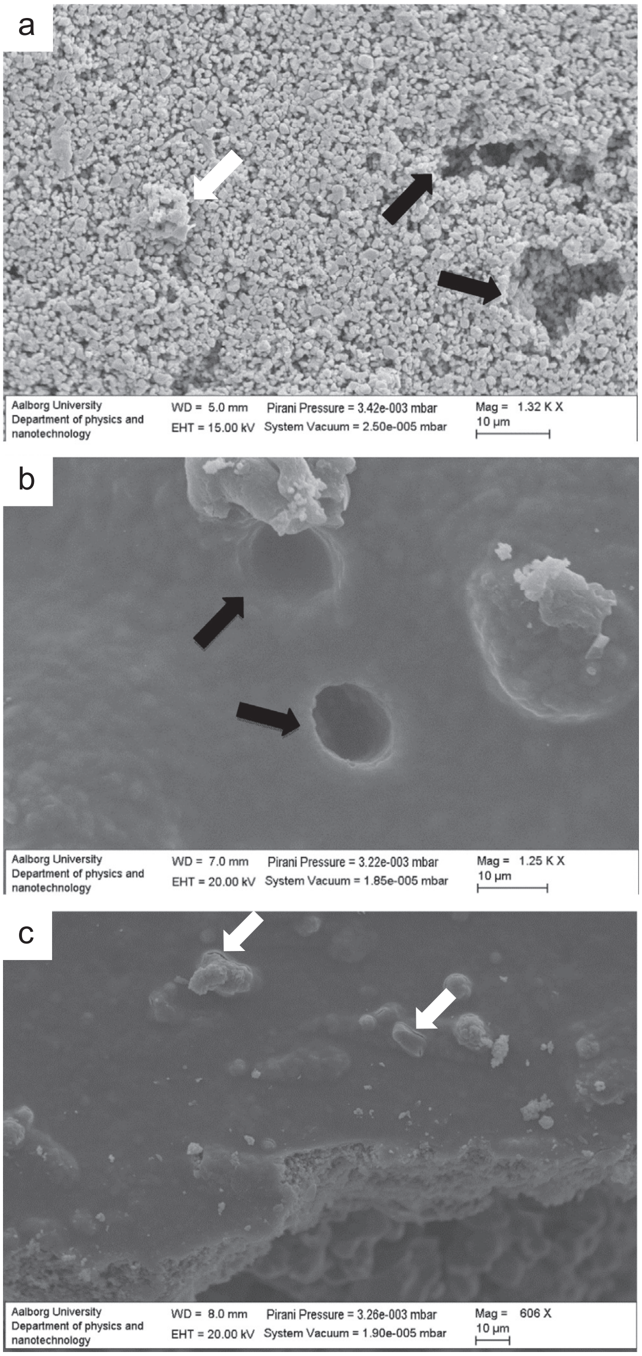

Fig. 10. Aggregates (white arrow) and craters (black arrows) on the surface of a SiC microfiltration tube (a), and defects in the coated γ-Al_2O_3 layer, occurring in the correspondence of the edges of this type of surface inhomogeneities (b) and (c).

4. Conclusions

In this work we have shown that continuous γ-Al_2O_3 layers can be deposited on the surface of commercial substrates with a surface roughness modulation of 0.2–1 μm. Multiple coatings allowed the reducing of the defect density in the deposited layers. By repeating the coating procedure five times, we obtained a 5.6 μm thick γ-Al_2O_3 layer, which showed a retention of ~75% for PEG molecules with theoretical hydrodynamic diameter of >4 nm. Therefore, our results indicate that, despite their intrinsic surface roughness, commercial SiC microfiltration tubes can be already applied as carrier for thin ultrafiltration membranes with enhanced water permeability. Despite that, the surface of these commercial supports typically presents a small number of inhomogeneities: craters with a depth larger than <1 μm, and SiC grains and aggregates with exceptionally high surface profile, which caused microcracks formation in the coated γ-Al_2O_3 membrane. Hence, our results point out that the development of fabrication techniques capable of avoiding inhomogeneities on the internal surface of SiC supports, could greatly enhance permeability and selectivity of this type of membranes, by allowing the deposition of thinner and defect-free γ-Al_2O_3 layers.

Acknowledgments

The financial support from the Danish National Advanced Technology Foundation (Project 0-59-11-1) is gratefully acknowledged. The authors wish to thanks Dr. Donghong Yu for his assistance during XRD analysis.

References

[1] V. Boffa, Fabrication of ultramicroporous silica membranes for pervaporation and gas-separation, in: B. Pignataro (Ed.), Molecules at Work, Wiley-VCH, Weinheim, 2012, pp. 177–205.

[2] H. Qi, S. Niu, X. Jiang, N. Xu, Enhanced performance of a macroporous ceramic support for nanofiltration by using α-Al_2O_3 with narrow size distribution, Ceramics International 39 (2013) 2463–2471.

[3] S. Abedini, N. Parvin, P. Ashtari, Preparation, characterization and microstructural optimization of a thin γ-alumina membrane on a porous stainless steel substrate, Materials Science and Engineering A 533 (2012) 1–8.

[4] L. Zhang, I.S. Park, K. Shqau, W.S.W. Ho, H. Verweij, Supported inorganic membranes: promises and challenges, Journal of the Minerals, Metals, and Materials Society 61 (2009) 61–71.

[5] H.J. Lin, W. Peng, M.J. Zhang, J.R. Chen, H.C. Hong, Y. Zhang, A review on anaerobic membrane bioreactors: applications, membrane fouling and future perspectives, Desalination 314 (2013) 169–188.

[6] M.T.M. Pendergast, E.M.V. Hoek, A review of water treatment membrane nanotechnologies, Energy and Environmental Science 4 (2011) 1946–1971.

[7] S. Sommer, T. Melin, Performance evaluation of microporous inorganic membranes in the dehydration of industrial solvents, Chemical Engineering and Processing: Process Intensification 44 (2005) 1138–1156.

[8] S.S. Ozdemir, M.G. Buonomenna, E. Drioli, Catalytic polymeric membranes: preparation and application, Applied Catalysis A 307 (2006) 167–183.

[9] J. Caroca, G. Villata, D. Fino, N. Russo, Comparison of different diesel particulate filters, Topics in Catalysis 52 (2009) 2076–2082.

[10] J. Dong, Y.S. Lin, M. Kanezashi, Z. Tang, Microporous inorganic membranes for high temperature hydrogen purification, Journal of Applied Physics 104 (2008) 121301.

[11] V. Boffa, J.E. ten Elshof, A.V. Petukhov, D.H.A. Blank, Microporous niobia-silica membrane with very low CO_2 permeability, ChemSusChem 1 (2008) 437–443.

[12] P. Malaviya, A. Singh, Physicochemical technologies for remediation of chromium-containing waters and wastewaters, Critical Reviews in Environmental Science and Technology 41 (2011) 1111–1172.

[13] L. Suarez, M.A. Diez, R. Garcıa, F.A. Riera, Membrane technology for the recovery of detergent compounds: a review, Journal of Industrial and Engineering Chemistry 18 (2012) 1859–1873.

[14] V. Jegatheesan, L. Shu, G. Keir, D.D. Phong, Evaluating membrane technology for clarification of sugarcane juice, Reviews in Environmental Science and Biotechnology 11 (2012) 109–124.

[15] P.A. Marichal-Gallardo, M.M. Alvarez, State-of-the-art in downstream processing of monoclonal antibodies: process trends in design and validation, Biotechnology Progress 28 (2012) 899–916.

[16] S. Ranamukhaarachchi, L. Meissner, C. Moresoli, Production of antioxidant soy protein hydrolysates by sequential ultrafiltration and nanofiltration, Journal of Membrane Science 429 (2013) 81–87.

[17] V. Demers-Mathieu, S.F. Gauthier, M. Britten, I. Fliss, G. Robitaille, J. Jean, Antibacterial activity of peptides extracted from tryptic hydrolyzate of whey protein by nanofiltration, International Dairy Journal 28 (2013) 94–101.

[18] R.J.R. Uhlhorn, M.H.B.J. Huis, In'T Veld, K. Keizer, A.J. Burggraaf, Synthesis of ceramic membranes. Part I. Synthesis of non-supported and supported gamma-alumina membranes without defects, Journal of Materials Science 27 (1992) 527–537.

[19] S. Alami-Younssi, A. Larbot, M. Persin, J. Sarrazin, L. Cot, Gamma alumina nanofiltration membrane. Application to the rejection of metallic cations, Journal of Membrane Science 91 (1994) 87–95.

[20] T. Kuzniatsova, M.L. Mottern, K. Shqau, D. Yu, H. Verweij, Microstructural optimization of supported γ-alumina membranes, Journal of Membrane Science 316 (2008) 80–88.

[21] K.S.W. Sing, D.H. Everett, R.A.W. Haul, L. Moscou, R.A. Pierotti, J. Rouquerol, T. Siemieniewska, Reporting physisorption data for gas/solid systems with special reference to the determination of surface area and porosity (recommendations 1984), Pure and Applied Chemistry 57 (1985) 603–619.

[22] A.L. Ahmad, C.P. Leo, S.R.A. Shukor, Tailoring of a γ-alumina membrane with a bimodal pore size distribution for improved permeability, Journal of the American Ceramic Society 91 (2008) 246–251.

[23] S.R. Chowdhury, R. Schmuhl, K. Keizer, J.E. ten Elshof, D.H.A. Blank, Pore size and surface chemistry effects on the transport of hydrophobic and hydrophilic solvents through mesoporous γ-alumina and silica MCM-48, Journal of Membrane Science 225 (2003) 177–186.

[24] H. Verweij, Ceramic membranes: morphology and transport, Journal of Materials Science 38 (2003) 4677–4695.

[25] K. Shqau, M.L. Mottern, D. Yu, H. Verweij, Preparation and properties of porous α-Al_2O_3 membrane supports, Journal of the American Ceramic Society 89 (2006) 1790–1794.

[26] M.L. Mottern, W.V. Chiu, Z.T. Warchol, K. Shqau, H. Verweij, High-performance membrane supports: a colloidal approach to the consolidation of coarse particles, International Journal of Hydrogen Energy 33 (2008) 3903–3914.

[27] K.Y. Lim, Y.W. Kim, I.H. Song, Porous sodium borate-bonded SiC ceramics, Ceramics International 39 (2013) 6827–6834.

[28] M. Herrmann, G. Standk, S. Höhn, G. Himpel, T. Gestrich, High-temperature corrosion of silicon carbide ceramics by coal ashes, Ceramics International (2013), in press, http://www.sciencedirect.com/science/article/pii/S0272884213008250.

[29] J.H. Eom, Y.W. Kim, I.H. Song, Effects of the initial α-SiC content on the microstructure, mechanical properties, and permeability of macroporous silicon carbide ceramics, Journal of the European Ceramic Society 32 (2012) 1283–1290.

[30] M.A. Bautista, J. Quispe Cancapa, J. Martinez Fernandez, M.A. Rodríguez, M. Singh, Microstructural and mechanical evaluation of porous biomorphic silicon carbide for high temperature filtering applications, Journal of the European Ceramic Society 31 (2011) 1325–1332.

[31] B. Hofs, J. Ogier, D. Vries, E.F. Beerendonk, E.R. Cornelissen, Comparison of ceramic and polymeric membrane permeability and fouling using surface water, Separation and Purification Technology 79 (2011) 365–374.

[32] X.H. Wang, Y. Hirata, Colloidal processing and mechanical properties of SiC with Al_2O_3 and Y_2O_3, Journal of the Ceramic Society of Japan 112 (2004) 22–28.

[33] B. Elyassi, M. Sahimi, T.T. Tsotsis, Silicon carbide membranes for gas separation applications, Journal of Membrane Science 228 (2007) 290–297.

[34] B. Elyassi, M. Sahimi, T.T. Tsotsis, A novel sacrificial interlayer-based method for the preparation of silicon carbide membranes, Journal of Membrane Science 316 (2008) 73–79.

[35] R. Rohani, M. Hyland, D. Patterson, A refined one-filtration method for aqueous based nanofiltration and ultrafiltration membrane molecular weight cut-off determination using polyethylene glycols, Journal of Membrane Science 382 (2011) 278–290.

[36] K.J. Kim, A.G. Fanen, R.B. Aim, M.G. Liu, G. Jonsson, I.C. Tessaro, A.P. Broek, D. Bargeman, A comparative study of techniques used for porous membrane characterization: pore characterization, Journal of Membrane Science 87 (1994) 35–46.

[37] J. Schaep, C. Vandecasteele, B. Peeters, Characteristics and retention properties of a mesoporous γ-Al_2O_3 membrane for nanofiltration, Journal of Membrane Science 163 (1999) 229–237.

[38] V. Boffa, J.E. ten Elshof, D.H.A. Blank, Preparation of templated mesoporous silica membranes on macroporous α-alumina supports via direct coating of thixotropic polymeric sols, Microporous and Mesoporous Materials 100 (2007) 173–182.

[39] H.C. Stumpf, A.S. Russell, J.W. Newsome, C.M. Tucker, Thermal transformations of aluminas and alumina hydrates-reaction with 44% technical acid, Industrial and Engineering Chemistry 42 (1950) 1398–1403.

[40] IUPAC recommendations, Reporting physisorption data for gas/solid systems with special reference to the determination of surface area and porosity, Pure and Applied Chemistry 57 (1985) 603–619.

[42] K.J. Kim, A.G. Fanen, R. Ben Aim, M.G. Liu, G. Jonsson, I.C. Tessaro, A.P. Broek, D. Bargeman, A comparative study of techniques used for porous membrane characterization: pore characterization, Journal of Membrane Science 81 (1994) 35–46.

[43] V. Boffa, D.H.A. Blank, J.E. ten Elshof, Hydrothermal stability of microporous silica and niobia-silica membrane, Journal of Membrane Science 319 (2008) 256–263.